Magnetic properties of slablike Josephson-junction arrays

D.-X. Chen
Instituto de Magnetismo Aplicado, RENFE-UCM, 28230 Las Rozas, Madrid, Spain

A. Sanchez
Grup d'Electromagnetisme, Departament de Física, Universitat Autònoma Barcelona, 08193 Bellaterra, Barcelona, Spain

A. Hernando
Instituto de Magnetismo Aplicado, RENFE-UCM, 28230 Las Rozas, Madrid, Spain
(Received 23 February 1994; revised manuscript received 23 June 1994)

Magnetic properties of infinitely long and wide slablike Josephson-junction arrays (JJA's) consisting of $2N+1$ rows of grains are calculated from the dc Josephson effect with gauge-invariant phase differences. When N is large, the intergranular magnetization curve, $M_J(H)$, of the JJA's in low fields approaches that of uniform Josephson junctions with lengths equal to the thicknesses of the JJA's, but in a larger field interval, its amplitude is dually modulated with periods determined by the junction and void areas. $M_J(H)$ curves for small N are more complicated. The concept of Josephson vortices and the application of the results to high-T_c superconductors are discussed.

I. INTRODUCTION

It is well known that sintered high-T_c superconductors (HTSC's) are granular in nature. Their intergranular matrix can be considered as a Josephson-junction (JJ) network. The properties of the entire network agree well with the critical-state model,[1] which was proposed to explain magnetic properties of conventional hard superconductors.[2] Since the coupling strengths between the grains have a large distribution, many HTSC's contain clusters, within which grains are more tightly linked by JJ's.[1,3–5] Inside grains, there may be subgrains which are even more tightly linked by JJ's.[6] Thus, precise knowledge of the magnetic properties of JJ's in different forms becomes very useful for understanding the magnetic properties of HTSC's.

We have calculated magnetic properties of uniform Josephson junctions (UJJ's) from both the sine-Gordon equation and a model array consisting of 41 short JJ's.[7,8] The results showed some interesting features: UJJ's can be magnetically reversible or irreversible, depending on the ratio of junction length to penetration depth to be less or greater than 4. The hysteresis loop of very long UJJ's is of surface-barrier type with quantitative difference from that of type-II superconductors (SC2's). The field-cooled magnetization can be diamagnetic, like the Meissner effect in SC2's, or paramagnetic at different fields. UJJ's may be an acceptable simulation to the JJ's between the subgrains or the well-matched large grains in the clusters, but they are quite different from the actual JJ assemblies in the network and most clusters, where the effect of voids is important.

In this work, we extend our calculation to Josephson junction arrays (JJA's). The magnetic properties of JJA's are not only determined by the JJ's linking the grains, but also influenced by the voids among the grains. Thus, they are closer to the situation of the intergranular network and clusters. Actually, as will be discussed later, JJA's still have different properties from the network, which is a disordered three-dimensional entity. They may be a good simulation to the clusters, whose sizes are smaller so that the effect of disorder is weak in each of them. For the sake of simplicity, we consider infinitely long and wide slablike JJA's, which are mathematically equivalent to real one-dimensional (1D) JJA's. Therefore, the results can be directly used for the latter, which are sometimes indeed the experimental arrangement.[9]

II. JJA MODEL AND MATHEMATICS

We consider a slablike JJA consisting of identical cylindrical superconducting grains parallel to the z axis, whose cross-sectional centers form a two-dimensional square lattice on the xy plane (Fig. 1). The lattice constant is a_0. The JJA is infinitely wide in the y direction,

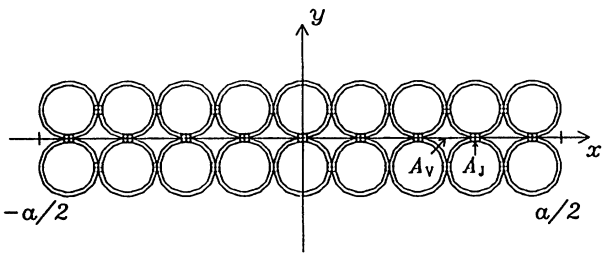

FIG. 1. Josephson-junction array schematic. From the infinite columns of grains only two are shown, each contains nine grains ($N=4$). The difference between the radii of concentric circles is λ_L.

and contains $2N+1$ rows (layers) along the x axis; thus the thickness of the array is defined as $a=(2N+1)a_0$. Magnetic field H is applied along the infinite length in the z direction, so that demagnetizing field is zero. We further assume that the JJ's between all the adjacent grains are short, with a maximum critical current $I_{\max}$ per unit length at zero field.

Under a uniform field H below the lower-critical field H_{c1} of the grains, two kinds of currents, circulating in the grains and through the JJA, appear. If we use an effective grain volume fraction f_g, by which the partial susceptibility of the grains themselves is adjusted to -1, only the currents circulating through the JJA need to be considered, which gives a partial magnetization M_J for the matrix. The matrix is defined as all the effective voids (including the space among grains and the grain shells of thickness λ_L, the London penetration depth) whose properties result from JJA-circulating currents. Owing to the infinite length and width, the currents flowing through the junction layers are uniform along the z axis and the fields produced by the currents have a z component only, which is also uniform along the same axis. Thus, the problem becomes one dimensional; only one column of junctions on the $y=0$ plane and the corresponding grains on its both sides have to be treated. We have

$$M_J=\sum_{k=1}^{N} I_{sk}(N-k+1)/(N+1/2), \tag{1}$$

where I_{sk} is the tunneling current per meter length across the junction for the kth (counted from the surface) layer.

To obtain N values of I_{sk}, a set of $2N$ nonlinear simultaneous equations has to be solved, since there are N phase differences for the layers being also unknown. To build up the equations we start from the dc Josephson equation for weakly linked superconductors, expressed by

$$I_s=I_{\max}\sin\theta, \tag{2}$$

where I_s is the supercurrent when the gauge-invariant phase (simplified as "phase" hereafter) difference across the junction is θ. Since each junction is short, Eq. (2) leads to a Fraunhofer diffraction pattern for the field dependence of critical current I_{ck} of the kth junction:

$$I_{ck}=I_{\max}\left|\frac{\sin(\pi\mu_0 H_{Jk}A_J/\Phi_0)}{\pi\mu_0 H_{Jk}A_J/\Phi_0}\right|, \tag{3}$$

where H_{Jk} is the average field acting on the kth junction, A_J is the effective junction area, equal to the junction length times thickness $d=2\lambda_L+t$, where t is the barrier thickness, and Φ_0 is the flux quantum. The real supercurrent flowing through the kth junction will be

$$I_{sk}=I_{ck}\sin\theta_k, \tag{4}$$

where θ_k is the average phase difference across the kth junction. Similar to a short or long junction, considering the gauge invariance, the phase relation between the kth and $(k+1)$th junctions is

$$\theta_k=-2\pi\mu_0 H_{Vk}A_V/\Phi_0+\theta_{k+1}, \tag{5}$$

where A_V is the area $(1-f_g)a_0^2$ of the effective void, which is bordered by the central lines of four nearest junctions around the void and includes the areas of depth λ_L in the four surrounding grains; H_{Vk} is the average field in the void between the kth and $(k+1)$th junctions.

H_{Jk} and H_{Vk} for $k=1,2,\ldots,N$ are calculated by

$$H_{Jk}=H+\sum_{j=0}^{k-1} I_{sj}+I_{sk}/2, \tag{6}$$

$$H_{Vk}=H+\sum_{j=0}^{k} I_{sj}, \tag{7}$$

where $I_{s0}=0$. Also, there is a zero induced current in the central $(N+1)$th layer, so that $\theta_{N+1}=0$.

After substituting Eqs. (3), (6), and (7) in Eqs. (4) and (5), a set of $2N$ simultaneous equations for $k=1,2,\ldots,N$ is formed. It is solved numerically by computer with a routine based on a modified Powell-hybrid method. Since the solution is generally multivalued, each calculation is performed starting from a first point and following a continuous curve. It is often needed to have several "first points" to complete an entire curve. Thus, all the I_{sk} and θ_k are obtained, from which M_J is calculated using Eq. (1).

III. MAGNETIC PROPERTIES OF JJA'S

A. Amplitude-modulated $M_J(H)$ curves

In the computation of M_J vs H curves, we assume $A_V=10A_J=10^{-11}$ m^2 and use different values of $I_{\max}$ and N. The obtained H and M_J are normalized to $\Phi_0/2N\mu_0 A_V$, $2NA_V$ being the total area of one column of voids. The normalized quantities are written as h and m_J:

$$h=2N\mu_0 A_V H/\Phi_0, \tag{8}$$

$$m_J=2N\mu_0 A_V M_J/\Phi_0. \tag{9}$$

Some calculated $m_J(h)$ curves are plotted in Figs. 2(a)–2(j). The same as for UJJ's, the curves for JJA's shown in Fig. 2 are oscillatory, which is a direct consequence of the sinusoidal function in Eq. (4). However, for JJA's, not only does m_J oscillate itself, but the amplitude of m_J also oscillates with greater periods. In other words, the $m_J(h)$ curves are amplitude modulated. There are two reasons for the modulation, the Fraunhofer diffraction pattern of short JJ's, Eq. (3), and the formation of multi-Φ_0 vortices or antivortices. This will be discussed below.

B. Penetration depth

Before further describing magnetic properties quantitatively it is necessary to introduce the Josephson pen-

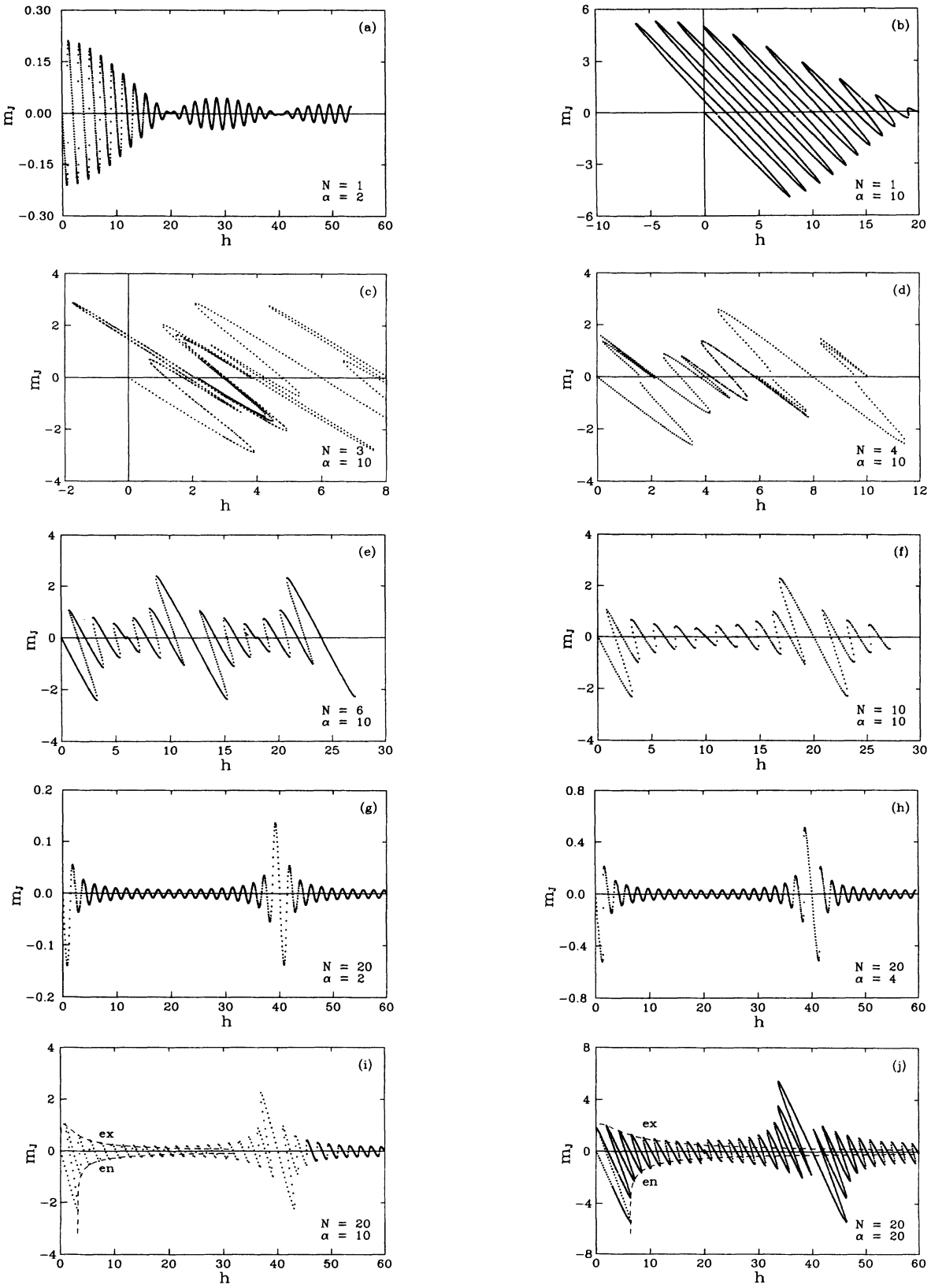

FIG. 2. Magnetization curves, M_J vs H, normalized to $\Phi_0/2N\mu_0 A_V$, of a Josephson-junction array for (a) $N = 1$, $\alpha = 2$; (b) $N = 1$, $\alpha = 10$; (c) $N = 3$, $\alpha = 10$; (d) $N = 4$, $\alpha = 10$; (e) $N = 6$, $\alpha = 10$; (f) $N = 10$, $\alpha = 10$; (g) $N = 20$, $\alpha = 2$; (h) $N = 20$, $\alpha = 4$; (i) $N = 20$, $\alpha = 10$; and (j) $N = 20$, $\alpha = 20$. Dashed lines in (i) and (j) display the Josephson vortex entry and exit magnetization curves calculated from Eqs. (15)–(18).

etration depth λ_J. λ_J is a characteristic parameter appearing in the sine-Gordon equation for UJJ's:[7]

$$\lambda_J = (\Phi_0/2\pi\mu_0 J_{\max} d)^{1/2}, \tag{10}$$

where $J_{\max}$ is the maximum critical-current density and $d = 2\lambda_L + t$, the same as given earlier for the JJA. When the UJJ is very long the internal field and current density at low applied fields will decay exponentially from its edges. λ_J is the depth at which they decrease to e^{-1} times their values on the surface. Similar decay also occurs in JJA's with large N and $I_{\max}$ at small H. The penetration depth λ_J is found to be

$$\lambda_J = a_0(\Phi_0/2\pi\mu_0 I_{\max} A_V)^{1/2}. \tag{11}$$

By comparison of Eq. (10) with Eq. (11), we find the correspondence between $J_{\max}$ and d in a UJJ and $I_{\max}$ and A_V in a JJA to be

$$J_{\max} \Longleftrightarrow I_{\max}/a_0,$$
$$d \Longleftrightarrow A_V/a_0.$$

For small N, the meaning of λ_J is not straightforward. In spite of this, we still use, like in the case of UJJ's, λ_J as a reference length scale for choosing calculation conditions and discussing the results. One of the calculation conditions for the curves given in Fig. 2 is the value of α, which is defined as the ratio of the effective JJA thickness to λ_J:

$$\alpha \equiv 2Na_0/\lambda_J. \tag{12}$$

C. Initial susceptibility

The initial susceptibility χ_{ini} is a characteristic quantity for all JJA's. The same as for UJJ's, if N is large, it can be calculated by[7]

$$\chi_{\text{ini}} = \frac{2}{\alpha}\tanh\frac{\alpha}{2} - 1. \tag{13}$$

With decreasing N, $-\chi_{\text{ini}}$ becomes smaller. $-\chi_{\text{ini}}$ as a function of N for $\alpha = 10$ is given in Fig. 3.

D. Reversible and irreversible JJA's

The same as for UJJ's, the $m_J(h)$ function for a JJA can be either singlevalued [Fig. 2(g)] or multivalued

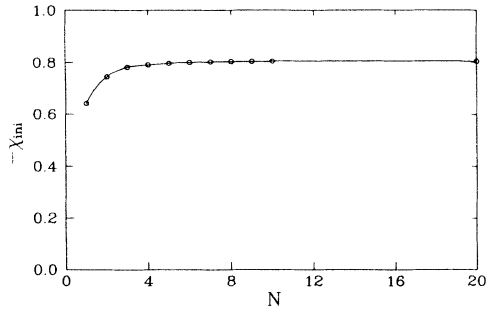

FIG. 3. Initial susceptibility as a function of N when $\alpha = 10$. The line is a guide for the eye.

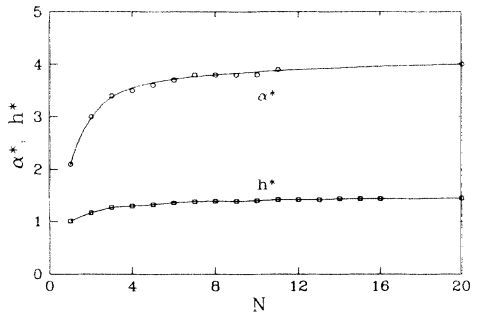

FIG. 4. The critical α, α^*, at which magnetic irreversibility sets in, as a function of N (open circles). h^* is the h for the m_J jump when $\alpha = \alpha^*$ (open squares). Lines are guides for the eye.

[Figs. 2(b)–2(f), 2(i), and 2(j)]. Therefore, if sweeping H forward and then backward, the resultant m_J vs h curve can be reversible or irreversible. The $m_J(h)$ curve of irreversible JJA's contains several pairs of m_J jumps if the maximum h is large enough. The starting and ending states for each jump are superconducting, but a "normal" state is in between, which gives rise to energy dissipation.

If N is large, the condition for the onset of irreversibility is

$$\alpha > \alpha^* = 4. \tag{14}$$

The critical α^* at which magnetic irreversibility sets in decreases to 2 with decreasing N to 1, as shown in Fig. 4. In Figs. 2(h) and 2(a) are plotted the curves for $N = 20$ and $\alpha = 4$, and $N = 1$ and $\alpha = 2$, representing two extreme critical cases.

E. Hysteresis loops

For irreversible JJA's, we can define a characteristic quantity h_1 as the h at which the first m_J jump takes place when increasing h from zero. This h_1 is the border of the low-field reversible h range for irreversible JJA's. With increasing α from 4 to ∞, h_1 for large N decreases from $1.16\alpha/\pi$ to α/π, equivalent to the change of the h_1 defined for UJJ's in Ref. 7 from 2.319 to 2. h_1 increases with decreasing N. Corresponding to h_1, there is h_2, the h at which the last m_J jump takes place during decreasing h. For $N \geq 4$, h_2 is positive, and it changes to negative at smaller N. h_1 and h_2 as functions of N are plotted in Fig. 5 for the case of $\alpha = 10$.

The number of the pairs of m_J jumps increases with increasing α. If α is very large, many small m_J jumps result in a big loop in a low-field region, beyond which there are several separated small loops. Further increasing h leads to a reversible field interval, after which irreversibility may arise again in the second modulation period [see Figs. 2(i) and 2(j)].

If N and α are very large, the big loop for the first modulation period can be well expressed by the vortex entry and exit curves calculated for very long UJJ's.[7]

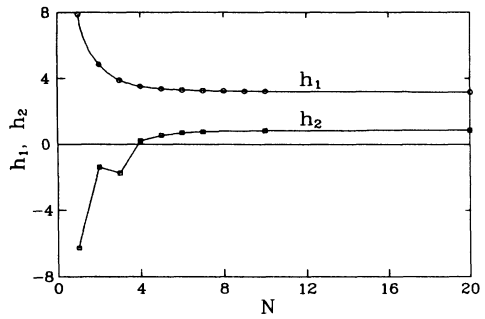

FIG. 5. The first field h_1 (open circles) for vortex entry during increasing h and the last field h_2 (open squares) for vortex exit during decreasing h as functions of N when $\alpha = 10$. Lines are guides for the eye.

Translating the formulas in Ref. 7 to the present case, we have the vortex entry and exit fields and magnetizations to be

$$h_{\rm en} = \alpha/\pi k, \tag{15}$$

$$m_{\rm en} = \alpha/2kK(k) - h_{\rm en}, \tag{16}$$

$$h_{\rm ex} = \alpha\sqrt{k^{-2}-1}/\pi, \tag{17}$$

$$m_{\rm ex} = \alpha/2kK(k) - h_{\rm ex}. \tag{18}$$

In these formulas, K is complete elliptic integral and its argument k changes from 1 to 0. The calculated $m_{\rm en}(h_{\rm en})$ and $m_{\rm ex}(h_{\rm ex})$ curves are plotted in Figs. 2(i) and 2(j).

For $N = 1$ and very large α, the big loop follows a tilted Fraunhofer diffraction pattern with the maximum width at $h = 0$, not of a surface-barrier type [see Fig. 2(b)]. For $2 \leq N \leq 5$, $m_J(h)$ curves do not have a regular shape [see Fig. 2(c) and 2(d)].

F. Field-cooled magnetization

The same as in the case of UJJ's,[7] the field-cooled magnetization of JJA's can be either diamagnetic or paramagnetic. With increasing h, the first transition from diamagnetic to paramagnetic occurs at $h = h^*$, where h^* is the h at which the m_J jump occurs when $\alpha = \alpha^*$. h^* as a function of N is given in Fig. 4.

Owing to the modulation of $m_J(h)$ curves field-cooled magnetization at higher fields has a series of maxima around $h = 2Ni$ $(i = 1, 2, \ldots)$. Paramagnetic and diamagnetic magnetizations occur at lower and higher field sides of $h = 2Ni$.

IV. DISCUSSION

A. JJA's and UJJ's

In the modeled infinitely wide slablike JJA there are no currents flowing along the x direction, or, the phase differences between the adjacent grains in each column remain zero. The calculated results should be the same as those for a real 1D-JJA, which consists of $2N+1$ short JJ's between two superconductors. This is because to calculate magnetic properties of 1D-JJA, only the phase differences between both superconductors need to be taken into account, which is mathematically equivalent to our slablike JJA. If N is large the current distribution in the 1D-JJA will approach a continuous one, similar to that in a UJJ. Therefore, our results for large N should be close to those of UJJ's.

B. Oscillatory and modulated $m_J(h)$ curves

However, there are still some important differences between our JJA's and UJJ's even if N is very large. An obvious one is the amplitude modulation of the magnetization curves.

Both oscillation and modulation in magnetization curves are the consequence of the sinusoidal function in Eq. (2). A period of oscillation or modulation signifies a 2π change in θ across a certain characteristic length along the x direction. Each length should be connected to an area where flux passes through. There are three such areas in the JJA's being, from large to small: NA_V, A_V, and A_J. The h change that gives rise to a Φ_0 of flux change in these three areas is 2, $2N$, and $2NA_V/A_J$, respectively. The first one is the period of the oscillation related to the entire JJA, so that it is common for JJA's and UJJ's. The other two are periods of two kinds of modulations related to A_V and A_J, therefore only for JJA's.

The trivial solution at $h = 0$ is $I_{sk} = 0$ and $\theta_k = 0$ for $k = 1, 2, \ldots, N$. In this case, the flux produced by h is zero everywhere. When $h = 2Ni$ $(i = 1, 2, 3, \ldots)$, $I_{sk} = 0$ should also be a solution. This is because such a current profile is consistent with a situation in which each void contains $i\Phi_0$ flux. Therefore, $m_J = 0$ at $h = 2Ni$, as seen from Fig. 2. Under our calculation condition of $A_V = 10A_J$ when each void contains $10i\Phi_0$ flux each JJ contains $i\Phi_0$ so that $I_{sk} = 0$ holds for all short JJ's, which is realized from Eqs. (3) and (4). Thus, the entire behavior of the $m_J(h)$ curve for large N will be as follows.

Starting from the initial state $(0, 0)$ and moving along the curve, m_J undergoes the first half oscillation with a maximum negative amplitude. The following $N-1$ oscillations have progressively decreasing and then increasing amplitudes, ending with a half oscillation of maximum positive amplitude terminated at the state $(2N, 0)$. This can be seen from Figs. 2(e)–2(j). This process is repeated in the following each N oscillations, the first of which can be seen from Fig. 2(e) completely. The maximum amplitudes in these modulated periods decrease monotonically until the state $(20N, 0)$, after which they increase and decrease again. We have not shown such a high-h behavior for large N, but it is similar to that shown in Fig. 2(a) for $N = 1$. Considering an entire h range from 0 to ∞, the maximum amplitudes of A_V modulation occurring around $h = (2Ni, 0)$ $(i = 0, 1, 2, \ldots)$ change their values by A_J modulation. The rule follows the Fraunhofer diffraction pattern; i.e., they are

the largest at $i = 0$, close to zero at $i = 10, 20, 30, \ldots$, and take progressively reduced maxima at $i = 15, 25, 35, \ldots$.

C. Josephson vortices

It has been shown in Ref. 7 that the magnetic properties of UJJ's can be entirely explained in terms of Josephson vortices (JV's) if the fractional JV's at both edges are also considered. There, JV is defined as a current vortex associated with a field peak whose total flux equals Φ_0. The similarity between JJA's and UJJ's suggests that the concepts of JV's can also be used for interpreting the properties of JJA's. In fact, within the first half of modulation period for JJA's of large N, i.e., for $|h| < N$, most statements given in Ref. 7 are valid with some changes.

In order to use the above definition of JV for JJA's, two modifications are needed.

(1) Only one column of JJ's is considered. In our JJA's, the net currents across JJ's along the x direction are all zero, and the currents along the y direction form closed paths through the infinity point. Therefore, each current vortex will enclose an infinite number of Φ_0's. To have its flux equal to Φ_0, one has to consider one column only, and to regard the zero current along the x direction as a cancellation of two equal currents with opposite directions. In fact, a current vortex associated with infinite Φ_0's is a consequence of our simplified model with an infinite width, and for JJA's with a finite width each JV should always contain one Φ_0 since the currents along the x direction do not remain zero but oscillate like those along the y direction. For the sake of simplicity, we will hereafter consider the JV's within one column only.

(2) Current vortices are associated with field peaks in a collective way. One can always divide the entire field profile into several peaks, each of which contains one Φ_0, since the field profile is continuous. The same division is often impossible for currents since they flow through discrete JJ's. In some cases, it is impossible to find a complete current vortex within a field peak. However, in the entire JJA one can find an integral number of current vortices associated with the same number of Φ_0's, which is a conceptual consequence of the dc Josephson equation and gauge invariance expressed by Eqs. (4) and (5).

Let us illustrate the above statements for the second modification by calculating field and current profiles for $N = 10$ and $\alpha = 10$. The results are given in Fig. 6. The magnetic states are chosen to be very close to $\theta_1 = 2\pi i$, $i = 1, 2, 3, \ldots, 10$. Their corresponding field profiles are shown in Fig. 6(a). In this figure, the internal field h_i in the kth void is h_{Vk}, and its change over JJ's is made sudden, since A_J is much smaller than A_V. Note that we have used a continuous variable k to stand for the x coordinate, $k = 11$ and 1 corresponding to $x = 0$ and $x = 10a_0 = 10a/21$, respectively. We observe that when $i = 0$, 5, and 10 the profiles are flat, which correspond to currents $I_s(k) = 0$. [The discrete expression I_{sk} has been changed into $I_s(k)$.] The cases $i = 1$, 2, 3, and 4 correspond to i field peaks. Although the peaks do not have the same shape for $i = 3$ and 4, each can always be defined containing a Φ_0. The solid circles in Figs. 6(b)–6(e) are the current profiles for $i = 1$, 2, 3, and 4.

Current vortices can be defined like in UJJ's for $i = 1$ and 2 but not for $i = 3$ and 4. For example, for $i = 2$, the two JV's are separated at $k = 6$ as realized from the two symmetric field peaks in Fig. 6(a), and we can easily see from the symmetric current profile in Fig. 6(c) that the net current is zero in each JV, i.e., the current in each JV forms a vortex. For $i = 3$, the three JV's defined by the field peaks in Fig. 6(a) are separated at somewhere between $k = 4$ and 5 and between $k = 7$ and 8. In this case as seen from Fig. 6(d), the net current within the middle field peak is zero but it is positive and negative within the left and right field peaks, respectively. Therefore, although the middle field peak contains a current vortex, the other two do not. However, three current vortices can be found if $I_s(4)$ and $I_s(8)$ are shared by two adjacent JV's. In this way, the borders for the three JV's will be located at $k = 4$ and 8, different from those defined above by the field peaks, so that the current-vortex and field-peak association can only be collective.

Because this second modification is complicated, we can also say that if JV is defined by a field peak containing a Φ_0, then JV's in JJA's are similar to those in UJJ's. Such a JV is actually a fluxon. In SC2's, the Abrikosov vortex is sometimes equivalently called the fluxon. Both names are identical, meaning a current vortex carrying a Φ_0 flux. In the JJA case, however, by JV one emphasizes the current vortex but by fluxon, the flux Φ_0.

We have described in Ref. 7 that JV's in UJJ's have the following three properties if the UJJ's are not subjected to a transport current: (1) The field carried by JV's always points in the direction of the applied field. (2) In uniform applied field, a JV can never form at the JJ center, and instead, JV's enter the JJ from both edges in pair. (3) There are neither distance nor overlap between two adjacent JV's even if one of them is fractional. After the modifications to the definition of JV's stated above, these properties are also valid for the JV's in JJA's. This can be realized by smoothening both the field and current profiles shown in Fig. 6. They are similar to those given in Ref. 7 for UJJ's, so that the JV's in JJA's should share most properties with JV's in UJJ's.

The state of $i = 5$ in Fig. 6 corresponds to $h = N$, where neither current vortices nor field peaks are present. Therefore, the similar properties between JJA's and UJJ's are limited to a field region of $|h| < N$, beyond which the differences between both systems are significant.

From Fig. 6(a) we see that there is a minimum JV size $2a_0$ in JJA's occurring at $h \approx N - 2$. When $h > N$, the vortex size increases again and equals Na_0 when $h \approx 2N-1$. This kind of size variation repeats periodically for $h > 2N$, with a period of $2N$. Another obvious feature of the field profiles is the symmetry with respect to the line of $h_i = N$. This has significant consequences to the definition and properties of JV's as follows.

Defining a field and current period as a JV (or more precisely, a fluxon), each JV for $N/2 < i < N$ will contain a field valley instead of a field peak, and contain $[(N + i)/(N-i)]\Phi_0$ instead of a Φ_0. Such JV's are not what are commonly recognized. To meet the traditional concept of

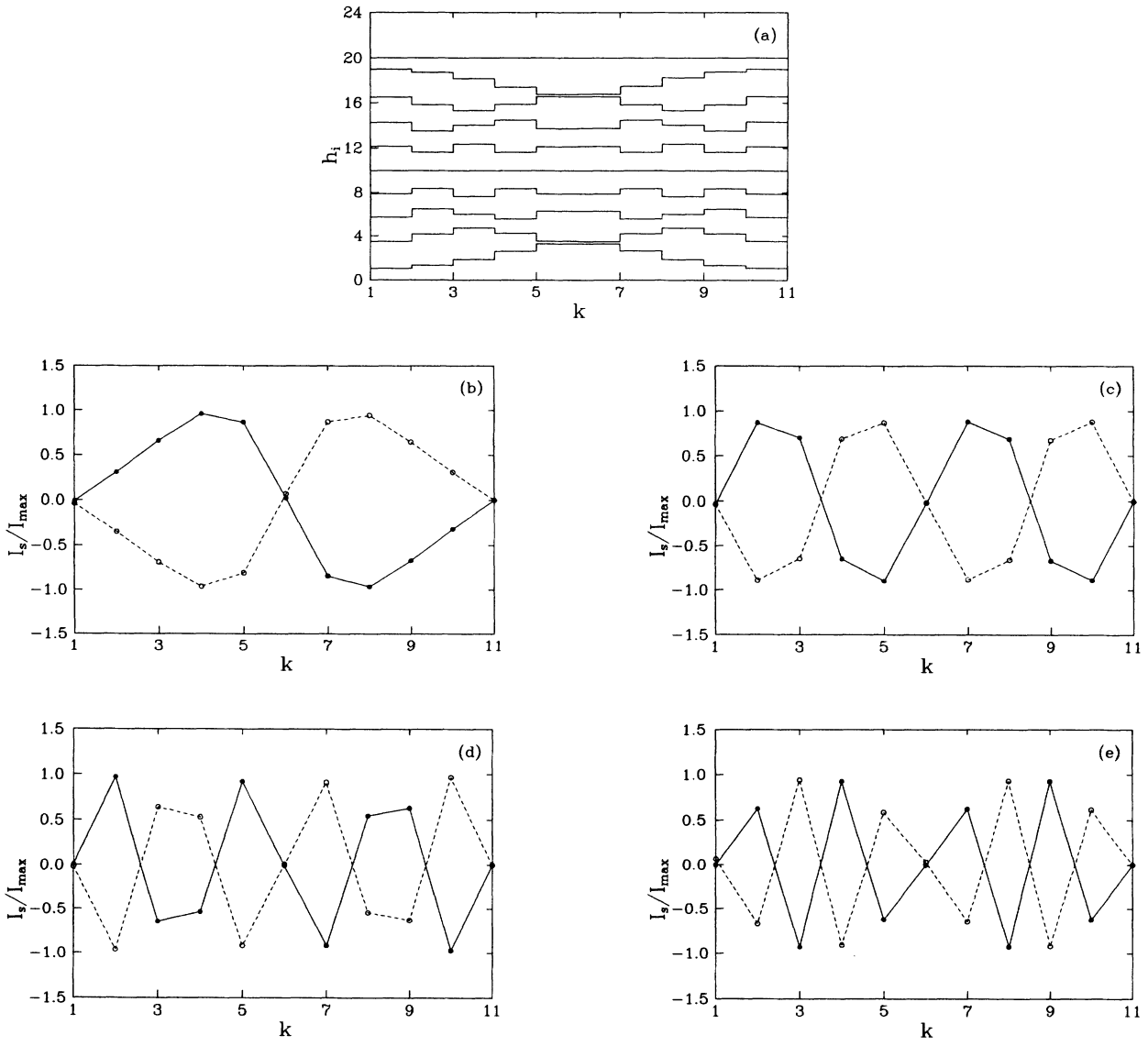

FIG. 6. (a) Internal field h_i and (b)–(e) current I_s/I_{max} profiles for $N = 10$ and $\alpha = 10$. The profiles for half JJA ($x \geq 0$) are presented. $k = 11$ corresponds to $x = 0$, and $k = 1$ is the position of the surface JJ layer. In (a) the curves from down to up are corresponding to $i = 1, 2, \ldots, 10$. In (b)–(e), the full circles are for $i = 1$ (b), 2 (c), 3 (d), and 4 (e) and the open circles for $i = 9$ (b), 8 (c), 7 (d), and 6 (e), respectively. The lines in (b)–(e) are guides for the eye.

JV corresponding to a Φ_0, we can define JV's in another way. If we change h_i to h_i' with $h_i = 2N + h_i'$, then the profiles of field h_i' of $i = N-1, N-2, \ldots, N/2+1$ will correspond to $-(N-i)\Phi_0$. The number of periods is $N-i$ in this case, which means that each period contains a $-\Phi_0$. Since the sign of flux associated with such JV's is opposite to that of the applied field, we can call these JV's anti-JV's. For anti-JV's, the corresponding current profiles are the negative of those of JV's, as given by the open circles in Figs. 6(b)–6(e). This second definition is consistent with the original definition of JV, but it has only formal meaning. To calculate the energy of a JV, the actual field h_i should be used but not h_i'.

In terms of the concepts of JV's and anti-JV's, the magnetization process can be interpreted as follows. With increasing h from the initial state, JV's enter from the JJA surface so that the number of JV's in the JJA increases successively; after $h = N$, JV's change into anti-JV's, and anti-JV's exit from the surface so that the number of the anti-JV's in the JJA decreases successively. This process of JV entry and anti-JV exit will repeat in the h intervals of $2N$-$4N, 4N$-$6N, \ldots$. On the contrary, with decreasing h, the entry of anti-JV's and exit of JV's occur in turn.

In the above we have considered N as an even number. The situation for an odd N is similar. The difference is that the flat h_i profile at $h_i = N$ will not correspond to a θ_1 equal to an integral number of 2π. Also, we only showed the profiles for integral i. If i is fractional, complexities will occur. Especially when N is small, such

complexities will lead to completely different magnetization behaviors.

D. Case of small N

The features described in Sec. IV B agree in general with most $m_J(h)$ curves given in Fig. 2. However, the situation is different when N is small. The $m_J(h)$ for $N \geq 4$ is a continuously forward curve (see the precise meaning of "forward" below), as seen from Figs. 2(d)–2(j). Starting from $(0,0)$, the curve passes through points $(N,0)$ and $(2N,0)$ as it should be, since at both points each void contains $\Phi_0/2$ and Φ_0 and provides a θ change of π and 2π so that all I_{sk} and $m_J = 0$. The curves for $N = 2$ and 3 are different. The calculated curves for $N = 3$ are shown in Fig. 2(c). Starting from $(0,0)$, the curve goes forward until a state $(3.8, 0.0)$, at which it turns backward. The backward section passes through $(N,0)$ and terminates at $(2.2, 0.0)$, after which the curve becomes forward again and finishes the period at $(2N,0)$. The entire curve contains rich harmonics with very sharp extra peaks and dips. This latter feature is also shown for $N = 4$ and 5 [see Fig. 2(d)]. As a consequence, h_2 becomes negative when $N = 2$ and 3, the corresponding points of which do not make a smooth curve when plotted together with those for $N \geq 4$ as seen from Fig. 5. With further decreasing N to 1, the oscillation period equals the lower modulation period, and we can see the A_J modulation only. h_2 becomes very close to $-h_1$ (Fig. 5), and the hysteresis loop follows tilted Fraunhofer patterns [Fig. 2(b)]. In other words, with decreasing N, the hysteresis loop of irreversible JJA's changes from a surface-barrier type to a tilted Fraunhofer type.

In UJJ's,[7] the $m_J(h)$ curve always goes forward, which means that the flux in the UJJ and the θ at the edge are always increasing with the continuous state evolution. The meaning of "forward" in JJA's is similar: the total flux in the JJA and the θ_1 increase with the continuous state evolution. On the contrary, "backward" means that they decrease. Therefore, a unique feature in the equilibrium magnetization of JJA's of $N = 2$ and 3 is as follows. Starting from the initial state $(0,0)$, a continuous state evolution involves periodically interchanged flux entry and exit from the JJA, which is distinct from the case of JJA's of larger N and UJJ, where only flux entry occurs.

The rich harmonics in the $m_J(h)$ curves for small N is consistent with the fact that JV defined by the current and field period does not exist in this case. The few A_V's in a column forbid any definition of JV. Finally, it is clear that if $N = 1$, the current can only circulate in the entire column $(-a/2 < x < a/2)$ and the field is always uniform in the entire JJA, so that either JV or its movements cannot be defined.

E. Application to HTSC's

Considering the application of our results to HTSC's, JJA's should be related to the intergranular matrix. This can be done through the average grain size a_0 and the effective grain volume fraction f_g. A_V is calculated from these two parameters using $A_V = (1 - f_g)a_0^2$, as mentioned in Sec. II. In the above computation, A_V is chosen as 10^{-11} m^2. Letting typically $f_g = 0.7$, a_0 is calculated to be 6×10^{-6} m, which is a typical average grain size for many HTSC's.

However, in order to compare our results with some existing works, we assume following Ref. 10 that $f_g = 0.7$, $a_0 = 10^{-6}$ m, and $I_{\max} = 100$ A/m. The last two quantities correspond to a current density $J_{\max} = 10^8$ A/m^2. Substituting these values in Eq. (11) we obtain $\lambda_J = 2.96 \times 10^{-6}$ m, consistent with the result given in Ref. 10. Applying standard Ginzburg-Landau theory for SC2's to JJA's and defining an effective coherence length $\xi_J = 0.5a_0$, the first field for JV entry is obtained to be 89 A/m in Ref. 10. (There is a slight difference in Ref. 11, where ξ_J is assumed to be $0.4a_0$.) For large N and α, this field is calculated from Eq. (15) by substituting $k = 1$ to be

$$H_1 = 2I_{\max}\lambda_J/a_0. \tag{19}$$

In the derivation of this formula, Eqs. (8) and (11) have been used. Substituting the above values in Eq. (19) leads to $H_1 = 592$ A/m, six times the result given in Ref. 10. The discrepancy between the SC2-JJA analogy and the direct JJA calculation suggests that there are essential differences between SC2's and JJA's; similar differences have been discussed in detail in Ref. 7 between SC2's and UJJ's.

An important deduction of the SC2-JJA analogy is that intergranular currents in JJA's containing defects should obey the critical state model, due to JV pinning.[10–12] Our calculation is carried out for uniform JJA's, but some features in the results should also be shown in nonuniform JJA's. The calculated magnetization curves for large N are of modulated surface barrier type, which are much different from the critical state loops given in Refs. 13–15. Nonuniformity will make the modulation less pronounced at high fields, but it will not change the surface-barrierlike feature. Actually, the current density is a function of local field in the critical state, whereas it is mainly a function of phase in JJA's, taking values within positive and negative maximum JJ currents. Changing the phase dominance to field dominance is the central problem in understanding the intergranular critical state. The JJA's we have treated are therefore not relevant for solving this problem; more work on intergranular critical state will be published elsewhere.

Grain clusters are more likely related to JJA's. Since they are formed of not many JJ's, their properties should be close to those of JJA's of small N. Thus, their hysteresis loop should not show a pronounced surface-barrier feature, but be close to a tilted diffraction pattern type. There may also be an anomalous field-cooled magnetization, even a paramagnetic Meissner effect if some π-JJ's exist in them.[16,17]

Surface-barrier effects occur in many HTSC's.[18–21] It is not always easy to explain them by the surface image force, since they are present in very small crystals and

even powders. Such effects could be related to intragranular JJA's. If this is true then modulated loops should be expected, which are similar to the fishtail phenomenon discovered in some HTSC's.[18,22,23]

V. CONCLUSION

Magnetization curves of slablike Josephson-junction arrays, which consist of $2N + 1$ layers of cylindrical superconductors of diameter a_0 weakly linked by short Josephson junctions, are calculated from simultaneous dc Josephson equations with gauge-invariant phase differences. When N is large, the results at low fields are similar to those for single uniform Josephson junctions, but the oscillatory magnetization is periodically modulated in a large field interval. In terms of h, the applied field normalized to $\Phi_0/2N\mu_0 A_V$, there are two kinds of modulations whose periods equal $2N$ and $2NA_V/A_J$, respectively, where A_V and A_J are the void and junction areas. α, defined by Eq. (12), greater than 4 for large N results in an irreversible magnetization; this critical α decreases with decreasing N and equals 2 when $N = 1$. If α is large, the low-field hysteresis loop is of a surface-barrier type for large N, with a positive last field h_2 for "vortex exit;" h_2 becomes negative when $N \leq 3$, and the surface-barrier type changes into one following tilted Fraunhofer diffraction patterns. In comparison with uniform Josephson junctions, Josephson vortices in JJA's become complicated; each vortex may contain more than one Φ_0 or become some kind of antivortex. These results may be applied to the grain clusters in HTSC's and might be related to other properties of HTSC's such as surface-barrier and fishtail effects in magnetization.

ACKNOWLEDGMENTS

We thank F. Lopez-Aguilar for support, and M. Coffey, R. B. Goldfarb, and A. Ustinov for their comments. We acknowledge financial support from Spanish CICYT through Project Nos. MAT91-0955, MAT92-0405, and MAT92-0491.

[1] D.-X. Chen and A. Sanchez, J. Appl. Phys. **70**, 5463 (1991).
[2] C. P. Bean, Phys. Rev. Lett. **8**, 250 (1962).
[3] D.-X. Chen, Yu Mei, and H. L. Luo, Physica C **167**, 317 (1990).
[4] D.-X. Chen, A. Sanchez, T. Puig, L. M. Martinez, and J. S. Muñoz, Physica C **168**, 652 (1990).
[5] J. W. Ekin, H. R. Hart, and A. R. Gaddipati, J. Appl. Phys. **68**, 2285 (1990).
[6] J. R. Clem, Physica C **162-164**, 1137 (1989).
[7] D.-X. Chen and A. Hernando, Phys. Rev. B **49**, 465 (1994).
[8] A. Sanchez, D.-X. Chen, and A. Hernando, Solid State Commun. **88**, 563 (1993).
[9] J. H. Miller, Jr., G. H. Gunaratne, Z. Zou, M. F. Davis, H. R. Rampersad, and J. C. Wolfe (unpublished).
[10] J. R. Clem, Physica C **153-155**, 50 (1988).
[11] M. Tinkham and C. J. Lobb, in *Solid State Physics*, edited by H. Ehrenr, F. Seitz, and D. Turnbull (Academic, New York, 1989), Vol. 42, p. 91.
[12] K.-H. Müller, Physica C **159**, 717 (1989).
[13] D.-X. Chen and R. B. Goldfarb, J. Appl. Phys. **66**, 2489 (1989).
[14] D.-X. Chen, A. Sanchez, and J. S. Muñoz, J. Appl. Phys. **67**, 3430 (1989).
[15] D.-X. Chen, A. Sanchez, J. Nogues, and J. S. Muñoz, Phys. Rev. B **41**, 9510 (1990).
[16] W. Braunisch, N. Knauf, V. Kataev, S. Neuhausen, A. Grütz, A. Kock, B. Roden, D. Khomskii, and D. Wohlleben, Phys. Rev. Lett. **68**, 1908 (1992).
[17] W. Braunisch, G. Bauer, A. Kock, B. Freitag, A. Grütz, V. Kataev, S. Neuhausen, B. Roden, D. Khomskii, and D. Wohlleben, Phys. Rev. B **48**, 4030 (1993).
[18] V. N. Kopylov, A. E. Koshelev, I. F. Schegolev, and T. G. Togonidze, Physica C **170**, 291 (1990).
[19] M. Konczykowski, L. I. Burlachkov, Y. Yeshurun, and F. Holtzberg, Phys. Rev. B **43**, 13 707 (1991).
[20] D.-X. Chen and A. Sanchez, Phys. Rev. B **45**, 10 793 (1992).
[21] D.-X. Chen, R. B. Goldfarb, R. W. Cross, and A. Sanchez, Phys. Rev. B **48**, 6426 (1993).
[22] M. Daeumling, J. M. Seuntjens, and D. C. Larbalestier, Nature **346**, 332 (1990).
[23] K. Kadowaki and T. Mochiku, Physica C **195**, 127 (1992).